Am. J. Hum. Genet. 57:8–21, 1995

Fifteen Novel *FBN1* Mutations Causing Marfan Syndrome Detected by Heteroduplex Analysis of Genomic Amplicons

Gaby Nijbroek,[1,2,3] Sumesh Sood,[1,2,3] Iain McIntosh,[2,4] Clair A. Francomano,[2,4] Evelyn Bull,[1,2,3] Lygia Pereira,[5,*] Francesco Ramirez,[5] Reed E. Pyeritz,[6] and Harry C. Dietz[1,2,3]

Departments of [1]Pediatrics, [2]Medicine, and [3]Molecular Biology and Genetics, Center for Medical Genetics, Johns Hopkins University School of Medicine, Baltimore; [4]National Center for Human Genome Research, National Institutes of Health, Bethesda; [5]Brookdale Center for Molecular Biology, Mount Sinai School of Medicine, New York; and [6]Department of Human Genetics, Allegheny-Singer Research Institute, Pittsburgh

Summary

Mutations in the gene encoding fibrillin-1 (*FBN1*), a component of the extracellular microfibril, cause the Marfan syndrome (MFS). This statement is supported by the observations that the classic Marfan phenotype cosegregates with intragenic and/or flanking marker alleles in all families tested and that a significant number of *FBN1* mutations have been identified in affected individuals. We have now devised a method to screen the entire coding sequence and flanking splice junctions of *FBN1*. On completion for a panel of nine probands with classic MFS, six new mutations were identified that accounted for disease in seven (78%) of nine patients. Nine additional new mutations have been characterized in the early stages of a larger screening project. These 15 mutations were equally distributed throughout the gene and, with one exception, were specific to single families. One-third of mutations created premature termination codons, and 6 of 15 substituted residues with putative significance for calcium binding to epidermal growth factor (EGF)–like domains. Mutations causing severe and rapidly progressive disease that presents in the neonatal period can occur in a larger region of the gene than previously demonstrated, and the nature of the mutation is as important a determinant as its location, in predisposing to this phenotype.

Introduction

The Marfan syndrome (MFS) is a systemic disorder of connective tissue with autosomal dominant inheritance and a prevalence of ~1 in 10,000 individuals. Approximately 25% of cases are sporadic, believed due to parental germ-line defects. In 1991 it was determined that mutations in *FBN1* can cause MFS (Dietz et al. 1991*a*). The corresponding gene product, fibrillin-1, is a 350-kD glycoprotein that contains many repetitive epidermal growth factor (EGF)–like subunits interspersed with transforming growth factor-β1-binding protein (TGF-β1-BP)–like domains (Lee et al. 1991; Maslen et al. 1991; Corson et al. 1993; Pereira et al. 1993). Fibrillin-1 monomers are constitutive components of extracellular microfibrils (Sakai et al. 1986). Multiple lines of evidence suggest that mutations in *FBN1* account for most, if not all, cases of MFS. First, the classic MFS phenotype cosegregates with intragenic or closely flanking marker alleles in all families tested (Kainulainen et al. 1990, 1991; Dietz et al. 1991*a*, 1991*b*; Lee et al. 1991; Tsipouras et al. 1991, 1992; Sarfarazi et al. 1992). Second, immunohistochemical analysis shows decreased extracellular fibrillin-1 in the vast majority of patient samples (Godfrey et al. 1990; Hollister et al. 1990). Third, with rare exceptions, a specific and reproducible defect in fibrillin-1 synthesis, secretion, or matrix deposition or in microfibrillar architecture is evident in patient samples (Milewicz et al. 1992; Aoyama et al. 1993, 1994; Kielty et al. 1994). Finally, *FBN1* mutations can even be found in samples that show a normal biochemical profile (H. Furthmayr, U. Francke, and H. C. Dietz, unpublished data).

In light of this compelling evidence that MFS is a monogenic disorder, the yield of mutation screening has been surprisingly low. On average, mutations have been identified in ~10% of screened patient samples (Byers 1993; Pyeritz and Francke 1993; Sykes 1993; Tynan et al. 1993). This poor performance has frustrated the use of mutational analysis for diagnostic purposes. It has also hampered efforts to correlate mutant genotype to clinical or cellular phenotype and, despite evidence to the contrary (Dietz et al. 1995), has even prompted speculation that MFS might show significant genetic heterogeneity (Collod et al. 1994).

Many factors may contribute to this low efficiency of mutation detection. *FBN1* is a large gene (~110 kb), and the coding sequence is highly fragmented (65 exons) (Pereira et al. 1993). Most investigators have relied on

Received February 14, 1995; accepted for publication April 24, 1995.

Address for correspondence and reprints: Dr. Harry C. Dietz, Division of Pediatric Cardiology, Ross 1170, Johns Hopkins Hospital, 720 Rutland Avenue, Baltimore, MD 21205.

*Present address: Instituto de Biociencias, Depto. de Biologia, University of Sao Paulo, Sao Paulo.

0002-9297/95/5701-0002$02.00

SSCP analysis of transcript-derived cDNA amplicons, a method whose efficiency varies in response to sequence context and DNA fragment size, that requires multiple running conditions in order to fully optimize sensitivity (Ravnik-Glavac et al. 1994), and that would be prone to miss premature termination codon (PTC) mutations that can be associated with low levels of mutant transcript (Urlaub et al. 1989; Cheng et al. 1990; Dietz et al. 1993*a*, 1993*b*).

In an attempt to optimize DNA fragment size and to eliminate the possibility of inefficient detection of reduced-transcript mutants, we have now designed a set of PCR primers that allow routine amplification of all 65 exons of the *FBN1* gene, including flanking splice sites, using genomic DNA as template. In that patients with MFS are predicted to be heterozygous for any given mutation, we investigated the suitability of heteroduplex analysis for mutation screening.

All 65 exons of the *FBN1* gene from nine unrelated probands with classic MFS were analyzed by heteroduplex analysis. Six mutations were identified that accounted for disease in seven (78%) of nine study participants. Our ongoing use of heteroduplex analysis has subsequently identified nine additional mutations. Five (33%) of 15 newly described mutations create premature signals for the termination of translation of mRNA. The spectrum of mutations that we have identified both complement and extend prior models regarding pathogenesis and early attempts to correlate mutant genotype to phenotype. We conclude that the enhanced mutation-screening sensitivity afforded by heteroduplex analysis of genomic amplicons will greatly assist both research efforts and the molecular diagnosis of families with MFS.

Subjects, Material, and Methods

Study Participants

The phenotype of all individuals assigned affected status satisfied the established diagnostic criteria for MFS (Beighton et al. 1988). Normal control subjects were unrelated and lacked any features of MFS.

Primer Design

Most primers used to generate PCR amplicons that span each exon of *FBN1* (table 1) were designed using intron sequences described elsewhere (Pereira et al. 1993). The goals were to include all *cis*-acting elements that participate in pre-mRNA splicing (Shapiro and Senapathy 1987) and to allow the use of the same primers for DNA amplification and sequencing. To this end, the 3′ nucleotide of nearly all primers is ≥20 bp from the splice junctions. In selected circumstances, the intronic sequences of Pereira et al. (1993) were extended by the sequencing of PCR products that spanned entire introns or of subcloned genomic fragments. We found that the sequence reported elsewhere for the 3′ end of intron 1 was erroneous because of the formation of a chimeric clone at the *Eco*RI site at position −23. The specificity of each primer pair for *FBN1* sequence was verified by the observed length and sequence of amplicons.

Mutation Detection

The standard PCR reaction (25 μl) contained 500 ng of genomic DNA, 0.2 mM each dNTP, 1.5 mM $MgCl_2$, 0.4 μM each primer, 1X PCR buffer and 1.25 U *Taq* DNA polymerase (Boehringer Mannheim). The thermal profile included denaturation for 8 min at 95°C, followed by 30 cycles of denaturation (30 s at 95°C), annealing (30 s at 54°C–60°C), and extension (30 s at 72°C), followed by a final step of extension (10 min at 72°C). Five microliters of each PCR sample were run on an agarose gel to confirm PCR amplification.

Mutation Detection Enhancement (MDE) gels (AT Biochem) were used to analyze PCR products for the presence of mutations in the *FBN1* gene. Five microliters of PCR product were combined with 1 μl of loading dye (50% [w/v] sucrose, 0.6% [w/v] bromophenol blue, and 0.6% [w/v] xylene cyanol). The samples were heated at 95°C for 3 min, slowly cooled to 37°C (5 min at 75°C, 5 min at 55°C, and 5 min at 37°C), and run on 0.5X MDE gels containing 0.6X Tris-Borate-EDTA (TBE). Gels were run overnight in 0.6X TBE at 225 V for 12–18 h, depending on the size of the PCR product. MDE gels were stained for 15 min at room temperature in a 1 μg/ml ethidium bromide, 0.6X TBE solution. Bands were visualized on a UV-transilluminator and photodocumented using the Eagle Eye system (Stratagene).

Mutations were characterized by direct sequencing of PCR products whenever a heteroduplex band was detected. Cycle sequencing was performed using the original primers and a commercial kit (BRL), according to instructions supplied by the manufacturer.

Population Screening

In the case of mutations leading to a PTC, only family members of the affected individual were analyzed. In the case of missense mutations, splice-site mutations, and in-frame deletions or insertions, family members and a minimum of 50 control subjects were analyzed. The methods used for population screening are shown in table 2. Restriction digestion was performed according to instructions supplied by the manufacturer of each specific enzyme. Restriction fragments were separated in 1% agarose (USB), 3% NuSieve (FMC BioProducts) gels and visualized after staining with ethidium bromide. Allele-specific oligonucleotide (ASO) hybridization analysis was performed as described elsewhere (Dietz et al. 1992*a*). The sequence and wash conditions for specific probes were C926R wild-type 5′-

Table I

***FBN1* Primers and Conditions for PCR**

Exon	Primer Sequences	Mg Concentration (mM) in a 10× Buffer	Position	Annealing Temperature (°C)
1S	GCA AGA GGC GGC GGG AG	5	−36 to +47	58
1AS	TGA AAC TTG GGA GAC CCA C			
2S	TCT GCC AGG ATT CAT CTT GC	15	−114 to +51	58
2AS	CAA CAC AAC AAA AGA AGG AC			
3S	TCG TGT TCC AAA TCC ATG TG	20	−46 to +51	58
3AS	TGG GTA TAA CCA CAT AAA ATA AT			
4S	AAC TCC TGT GAG CTG TTG C	15	−69 to +106	58
4AS	GCT GTG TCC CAG GTA ATC G			
5S	TCA GGT AAA GCG TCT CAG C	15	−38 to +49	58
5AS	ATC CCG GGT ACC AGC ATG			
6S	TCT GCA TGA TGG TTC CTG C	15	−60 to +50	58
6AS	CCA GAG CAA ATA AGA TTA ATC C			
7S	TCT GCA ATG AAT TTC ATA TGA G	15	−59 to +48	58
7AS	ACT ACA CCC CCC AAC TGC			
8S	ACT GAC GAA TGG TTT TAT ATT G	15	−61 to +37	58
8AS	TAC ACA AAC CAT GCA TGC TG			
9S	GTT ACA AGT ATT ATC TCA GCG	15	−55 to +42	58
9AS	GCT GGG ATG GGA TAT TCT G			
10S	CAG CTG TTG TGT TTT GTT TTG	15	−35 to +53	58
10AS	ATG TTA ACT TGA ACA ATG CAA G			
11S	ACT GAT GAA AGA TAC CAT AGT T	15	−56 to +52	58
11AS	AGG AAC AGA ATT ACA ACA GAC			
12S	AGA ATT ATG AGG TAT TGC TAT G	15	−55 to +48	58
12AS	CAG TTA GCA TAT ATG TCC CAC			
13S	TCC CCC AAA TAA AGC TAT TTC	20	−44 to +48	56
13AS	TGA AAC TGC AAT GGA AGG AG			
14S	TCA GGT CAT AAG AAA ATG TAT G	15–20	−36 to +51	58
14AS	GGA GGA GAA AAG GCA CGT G			
15S	TGT CAC TTC ATT TTT AAT AAG TG	15–20	−39 to +59	58
15AS	GTG ACA GAG GCT GAA CCT C			
16S	CTC ATC TGT TTG AAG TGA CAG	15	−50 to +48	58
16AS	GGT GGC AGA AGG CTG GC			
17S	GAT CTA CCT GTT CTG CAA AC	15–20	−55 to +24	58
17AS	GTA AAT TTT GAA AGG AAT CCT TA			
18S	TCA GAA TAT CCT TAC AGT GAG	15	−158 to +91	58
18AS	TCT AAG CTA CTC AAA GGC AG			
19S	AAA GTT TGG GCC CTT TTT AAG	15	−45 to +40	58
19AS	ATA GCA AAG TAC ACA GTA TAA G			
20S	CCC AGA CTA GAT TTT AGC AG	15	−46 to +56	58
20AS	TTA AGT ATA ACA ACA TTG ATA AAC			
21S	GTG TAT GTT TGA ATT TTT ATA TAG	15	−55 to +95	58
21AS	CTC ATG TGA GCC TAG ATA AAT G			
22S	CTA CTT CAT GCT CCA GGT C	15	−114 to +146	58
22AS	CTG TTC CGT TTT GTA GTT CTC			

(*continued*)

Table I (continued)

Exon	Primer Sequences	Mg Concentration (mM) in a 10× Buffer	Position	Annealing Temperature (°C)
23S	GTT TTA TGA ACT TAC CAG GTT C	15	−113 to +94	58
23AS	ACC GAA GCT AAG TGC TCA G			
24S	CAG CAA ATT ATT ATG TGT GCA G	15	−105 to +85	58
24AS	ATC AAG TAG AGT GCT GAG ATC			
25S	CAA GAA CTT CCA ACC TTC ATG	15	−101 to +46	58
25AS	TTA AAG GAC GTC CCC TCT C			
26S	AAT TAA GGC TGT CCT GAG AC	15	−51 to +47	58
26AS	CAT GGA ATC CTT CTC TTT CTG			
27S	GGC CCC CAC CTT TAA CAT G	15	−37 to +19	54
27AS	GAA AGT CTT TGC TCC TTA C			
28S	TGC CAA AGT TGG AAG CTT ATG	15	−54 to +45	58
28AS	TAA CAT AAC ATA ACA TAA AAT AAA G			
29S	CAG ACA TCC AAA CCA TAT CAG	10–20	−49 to +41	58
29AS	GAA CCT ACT GAG AGA TTC AAC			
30S	AAT AGT CTT ATG CTA GTA GGC	15	−113 to +53	58
30AS	ACA GTG CTT ATG ACT AAC AAG			
31S	GTA CTC AAT GAT ATC AAA TAG C	15	−53 to +51	58
31AS	ACC AAT CTC TTA ACT ACT TAA TA			
32S	CCA AAA GAC ATT TGT GCT GAG	15	−52 to +51	58
32AS	GTG TAA TCT ATG CAG TCC TTG			
33S	GGT TTT AAA TAC CAC CCT TTC	20	−52 to +49	58
33AS	CTG GCT TCT CTG ACT AGT G			
34S	CGA GGA AGA GTA ACG TGT G	15	−35 to +41	58
34AS	TCA AGC CCA GCA AGG CTC			
35S	AGT TTT TGC TTT TTC TCC CTC	5	−29 to +43	58
35AS	CGG GAC ACC AGG GAG CTG			
36S	GAG ATA ACT CCA CTA CTC AC	15–20	−33 to +45	58
36AS	AAT ACA CAG TAT GCT TGC TTC			
37S	GTA GAA AGA TTC TGC CTG ATG	15	−47 to +48	58
37AS	GAA CTG GCT GGA GTT GAA AT			
38S	AAA CTT TAG ATT CAA AAC AAC TC	15	−46 to +40	58
38AS	TCA AGT TGT GTG TGC TTT AAG			
39S	ATT TAC AAT GCT AAA GGA ATG C	20	−42 to +49	56–58
39AS	TCA GTT CTT GAT ATC TGC AAG			
40S	AAA TGT GAA GTT TTC ATA TTC AC	15	−48 to +30	58
40AS	CAT GCA TTA CTG AGA AAA GCT			
41S	GCT TGT TGA GTA TCC ACT TAG	15	−88 to +86	58
41AS	GCT TCC TTC GCT AAG ACT G			
42S	TAT CCT CCG GTC CCA CCT	15	−35 to +35	58
42AS	AAC CAG AAA GTT CTG ACA ATG			
43S	TGT CCT GTC ACT CAT GAA TG	15	−36 to +38	58
43AS	CTC TTT TCT GGA TAT GAT AAA G			
44S	CTG TTC TCC TTC AAA TTC AGT	15	−37 to +33	58
44AS	GTA GGC ATG TCC AGC CTG			

(*continued*)

Table I (continued)

Exon	Primer Sequences	Mg Concentration (mM) in a 10× Buffer	Position	Annealing Temperature (°C)
45S	GAG CTA GGA TTA CTC CTG AG	15	−95 to +141	60
45AS	CTG CTG CAT ATC TGT CTG TG			
46S	AAG TTC TCA GCC TAT GGA TG	15	−118 to +82	58
46AS	TGG TTC ACT AGA GAT GAT GC			
47S	GAC ATC TTT GGA ATA TAT TAA AG	20	−47 to +27	56
47AS	CCA GGT CTT TCT AAG TCC TG			
48S	GAT GGA AGT CAT GCC AGT G	5	−54 to +45	58
48AS	GGA CAC CCG ACA CTC CTC			
49S	TGA TGT CTC CAT CGT GTT TG	20	−49 to +57	56–58
49AS	AGA CCA CCA CAA ATA AAC ATG			
50S	ACG GAC TCA GTA GGA AAG C	15	−50 to +49	58
50AS	CAG TCT GCA CCC TGC ATG			
51S	AGC TTG TAA TGA ATT GCT ATT G	15	−53 to +52	58
51AS	AAG CAG ATT GAG AAT ACT GAG			
52S	TTG TCC CTT CAT TTA GAT AGC	15	−135 to +162	58
52AS	CCT GAT GGT GAC TCA CTA G			
53S	CTC AAT TCA TCA TGT TTT GGA C	15	−42 to +126	58
53AS	CCA TCA GGC CTA GAT GAT C			
54S	CTT TGT TGC TGT CCA TGA TC	15	−49 to +50	58
54AS	CTC ACA GAT AAA GCT TCC TG			
55S	GCA GAT ATA TGC ATT TTC TTT G	15	−51 to +53	58
55AS	GTC CAC TGT CAC TTC TGA TG			
56S	TGG TCA GAT GAC TCT TCT TG	15	−48 to +45	58
56AS	GTG TGG AGG CTG AGG TTA G			
57S	ATT TCC TGA CAT CCC CTT TG	15	−40 to +48	56
57AS	CAA ATA AAT AGA TTC CCT GTA AG			
58S	CAC TGA AGT GAC CCC CTA C	20	−76 to +41	58
58AS	AAT TTC CAC TTG AGG ATA AGC			
59S	GCG TGT ACA CAT CAT TTT TAG	15	−54 to +45	58
59AS	ATG TGT CAG GAG CTA GGT G			
60S	ATC CTG TTT TGT TGG CTG AC	15	−49 to +43	58
60AS	GAA TCG CTA CAA TCC ATG TAG			
61S	GTA TGT GTG AGC ACA CCT G	20	−148 to +47	58
61AS	CTC CAC AAG GAT TCA CCA G			
62S	AGA GAT GTT GAG TTG GCA TC	15	−44 to +47	58
62AS	TAG GAC CTG ATA GCC ATG C			
63S	CAA GTG GCC AGA TCC AAT G	5–20	−75 to +101	58
63AS	GGT TCT CCT CTG CTA GGA C			
64S	CCT ACC TTG TCT TCC CAT TC	15	−55 to +114	58
64AS	AGT TTC TCC CTG GGG AGC			
65S	GAG CTA AGT GGC ATA TGT AC	15	−54 to +98[a]	58
65AS	TGT ACC TAT GAT ATG ATG ATT C			

[a] Counted from the 1st nt of the termination codon.

Table 2

Novel *FBN1* Mutations

Nucleotide Change	Amino Acid Change	Exon	Exon Type[a]	Inheritance	Phenotype[b]	Screening Method[c]
G386A[d]	C129Y	4	EGF (ncb)	Sporadic	S, A	MDE and sequencing
G497T	C166F	5	EGF (ncb)	Sporadic	C, A	ASO
1604 delT	Frameshift	13	EGF (cb)	Familial	C	MDE and sequencing
A2237G[d]	Y746C	18	EGF (cb)	Sporadic	C	MDE and sequencing
T2776C[d]	C926R	23	EGF (cd)	Familial	C	ASO
G3037A[d]	G1013R	24	TGF	Sporadic	S, A	Loss *Nci*I site
G3217A	E1073K	26	EGF (cb)	Sporadic	S, A	Loss *Bsm*I site
del3901-4;3908-9[d]	del1301-1303;insH	31	EGF (cb)	Sporadic	S, A	MDE and sequencing
4020 delC	Frameshift	32	EGF (cb)	Sporadic	C	MDE and sequencing
A4145G	N1382S	33	EGF (cb)	Familial	C	Gain *Rsa*I site
4857 delA	Frameshift	39	EGF (cb)	Familial	M, V	Loss *Mnl*I site
T5782C	C1928R	46	EGF (cb)	Familial	C	ASO
Intron 46 G+5 to A[d]	Exon skipping/ cryptic splice site	46	EGF (cb)	Sporadic/recurrent	C	Gain *Nla*III site
C6784T	Q2262X	55	EGF (cb)	Familial	C	MDE and sequencing
8236 delGA	Frameshift	65	Carboxy	Sporadic	M, A	MDE and sequencing

[a] EGF = EGF-like; TGF = TGF-β1-BP–like; cb = calcium binding; and ncb = non–calcium binding.

[b] C = classic involvement of the ocular, skeletal, and cardiovascular systems; S = severe and rapidly progressive disease presenting in the neonatal period (see text); A = atypical manifestations (see text); M = mild disease (see text); and V = intrafamilial variability (see text).

[c] ASO = ASO hybridization analysis; and MDE = MDE heteroduplex analysis.

[d] Mutations found during the screening of the original panel of nine unrelated probands.

AATGGCCTGTGTGTTAACAC-3′, mutant 5′-AATGGCCTGCGTGTTAACAC-3′, final wash at 60°C; C166F wild-type 5′-CCAAATCGATTTGCATGCAC-3′, mutant 5′-CCAAATCGATGTGCATGCAC-3′, final wash at 58°C; and C1928R wild-type 5′-GCACCTATACAGTCATTGTT-3′, mutant 5′-AACAATGACCGTATAGGTGC-3′, final wash at 58°C.

Reverse Transcription (RT)-PCR and Transcript Quantification

Fibroblast cell culture, RNA isolation, and RT were performed as previously described (Dietz et al. 1992*a*). The RT-PCR assay for the skipping of exon 46 used a sense primer complementary to exon 44 sequence (5′-ATGCATCAACACTGCAGGC-3′) and an antisense primer complementary to exon 48 sequence (5′-GACCCATCCAAGTTTTGACA-3′). Both RT-PCR products that manifest abnormal splicing were cloned into the pCRII vector (Invitrogen) and sequenced in entirety. Quantification of the relative contribution of the wild-type and mutant alleles to the total *FBN1* transcript pool for mutations 4857delA and 8236delGA used described methods (Dietz et al. 1993*a*) and ASOs: 4857delA wild-type 5′-ACATTTTCCTCCTTGGCA-3′, mutant 5′-TACATTTTCCCCTTGGCA-3′; 8236delGA wild-type 5′-GATCAGTCTGAGACAGAAGC-3′, mutant 5′-GATCAGTCTGACAGAAGCCA-3′.

Results

Heteroduplex analysis allowed the detection of all previously characterized mutations that were tested ($n = 6$; data not shown). In a panel of nine unrelated probands for whom all 65 exons have been screened, six novel mutations were characterized, accounting for the disease phenotype in seven (78%) of nine participants (table 2). Identical methods are now being applied to a much larger group of patient samples ($n = 40$). To date, an additional nine novel mutations have been characterized. This panel includes samples that are at many different (and incomplete) phases of screening. In addition, many patients have truly atypical phenotypes that are associated with variable levels of confidence that the primary genetic defect is in *FBN1*. Therefore, the data derived from this panel cannot yet be used to estimate the efficiency of our methods for mutation detection. During the course of mutation screening, 13 polymorphisms were identified (table 3). Representative examples of shifted bands detected during heteroduplex analysis are shown in figure 1.

Characteristics of the 15 novel mutations that were identified in this study are shown in table 2. In general, each mutation showed complete cosegregation with the assignment of affected status in individual families and all cases of sporadic disease were associated with de novo mutational events (data not shown). The sole exception was identified on analysis of the family segregating a mutation that substitutes arginine (R) for cysteine (C) at codon 926 (C926R) within a calcium-binding EGF-like domain. Family and population studies were performed using ASO hybridization analysis. While most family members assigned affected status had classic

Table 3

Novel *FBN1* Polymorphisms

Polymorphism and Nucleotide Change	Amino Acid Change	Exon	Heterozygosity[a]
Coding sequence polymorphisms:			
A6849G	None	55	
T6855C	None	55	.14
G6888A	None	56	.14
C8202T	None	64	
	Intron		
Intronic sequence polymorphisms:			
Exon 18 −46 (A/G)	17		.43
Exon 24 +7 del T	24		
Exon 28 +15 del TTTTA	28		.33
Exon 41 −35 (C/T)	40		.125
Exon 41 −14 ins T	40		.125
Exon 45 +22 ins T	45		
Exon 52 −85 (T/A)	51		
Exon 56 +17 (G/C)	56		
Exon 63 −21 (C/T)	62		

[a] Reported only if variant was seen in more than one unrelated individual.

MFS and carried mutation C926R, the manifestations in one individual were limited to scoliosis, palate deformity, and mitral valve prolapse. Satisfying the clinical diagnostic criteria for MFS (Beighton et al. 1988), this individual decided not to have children. Mutation segregation analysis, however, clearly demonstrates that she did not inherit the mutation associated with classic MFS in her extended family (fig. 2).

The 15 new mutations identified in this study fall into many different classes (table 2). Eight (53%) are missense mutations. Seven substitute residues that are highly conserved in EGF-like domains found in *FBN1* and in other proteins (Maslen et al. 1991; Corson et al. 1993; Pereira et al. 1993). Five of seven occur in EGF-like domains that satisfy the consensus for calcium binding (Handford et al. 1991). One missense mutation (G1013R) substitutes a glycine residue in a TGF-β1-BP–like domain. One mutation (del1301-1303; insH) involves the deletion of nt 3901–3904, followed by the deletion of nt 3908–3909. The net result is the loss of three residues, glycine (G), serine (S), and phenylalanine (F) at codons 1301, 1302, and 1303, respectively, with the addition of a histidine (H) residue at position 1301. Another mutation (intron 46 G+5 to A) substitutes a conserved residue within the mammalian splice donor consensus and causes exon skipping. Five mutations (33%) create a PTC, four frameshift mutations and one nonsense mutation. Four premature signals for the termination of translation of mRNA occur prior to the penultimate exon of *FBN1,* and would therefore be predicted to effect degradation of the mutant transcripts (mutations 1604delT, 4020delC, 4857delA, and Q2262X). Mutation 8236delGA creates a PTC in the last exon of *FBN1;* mutant transcript would therefore be predicted to be spared from degradative pathways (Cheng et al. 1990). Indeed, mutation 4857delA was associated with steady-state mutant *FBN1* transcript abundance that was only 10% of that from the wild-type allele (data not shown). In contrast, wild-type and mutant *FBN1* transcripts were equally represented in a cell line harboring mutation 8236delGA.

The phenotype associated with 8 of 15 mutations described here showed classic involvement of the ocular, skeletal, and cardiovascular systems (table 2). In contrast, four mutations were identified in individuals who manifested severe and rapidly progressive disease that presented in the neonatal period. All had sporadic disease and de novo mutational events. Mutation C129Y was identified in a patient who was diagnosed at birth with joint contractures, pectus excavatum, bilateral inguinal hernia and ectopia lentis, restricted mouth opening, downward palpebral fissures, and a beaked nose. Karyotype analysis was normal. The child was subsequently diagnosed with spontaneous pneumothorax, retinal detachment, staining of the tooth enamel, mitral valve prolapse with regurgitation, and progressive aortic root dilatation. Mutation G1013R was found in a patient with atypically severe disease characterized by neonatal presentation with panvalvular dysfunction, gross aortic dilatation, congestive heart failure, crumpled ears, ectopia lentis, and severe skeletal deformity including marked joint contractures. Her clinical course has

included mitral valve replacement, surgical repair of ascending and descending aortic dissections, and multiple orthopedic surgeries. At age 15 years, she is functionally crippled because of circulatory insufficiency and a combination of devastating joint laxity and contracture. The patient carrying mutation E1073K was diagnosed in the neonatal period on the basis of extreme dolichostenomelia, arachnodactyly, scoliosis, joint contractures, crumpled ears, progressive aortic root dilatation, and mitral valve prolapse. Finally, the patient with mutation del1301-1303; insH was diagnosed at birth with severe skeletal and cardiovascular manifestations that necessitated mitral valve replacement, aortic root repair, and multiple orthopedic surgeries in early childhood.

Other mutations were associated with atypical manifestations or a mild disease phenotype. Mutation C166F was found in a patient with classic MFS compounded by severe aneurysmal disease involving the ascending thoracic, descending thoracic, and abdominal aorta and the carotid, pulmonary, renal, and iliac arteries. In the family segregating mutation 4857delA, the natural history of the disorder shows considerable variability among affected family members. The father underwent repair of an abdominal aortic aneurysm as a young adult, and subsequently required prophylactic replacement of his aortic root in his 6th decade of life. Both adult daughters had minimal and slowly progressive aortic root dilation. Only the father had lens dislocation, which was extremely mild. All affected family members were concordant for mitral valve prolapse with regurgitation, striae distensae, bone overgrowth, most pronounced in the feet, and a distinctly non-asthenic body habitus. Finally, mutation 8236delGA was found in a patient with sporadic, atypical, and mild MFS. While the patient was tall and had hyperextensible joints, myopia, anterior chest deformity, striae distensae, and mitral valve prolapse, she did not demonstrate arachnodactyly, long extremities, or ectopia lentis. The aortic root dimension was borderline-normal when standardized to age and body surface area. Truly atypical findings included translucent skin with "cigarette paper" scars, a large hyperpigmented region over the anterior abdominal wall and severe proptosis requiring multiple surgical procedures. Thyroid function studies were normal.

Prior to this study, only 1 *FBN1* mutation had been found to be recurrent among unrelated individuals (Dietz et al. 1991*a*). A second recurrent mutation has now been identified. Analysis of PCR products from the nine probands in our original panel revealed the same DNA-migration abnormality in the samples from two unrelated patients with sporadic and classic MFS. Direct sequencing revealed a G-to-A transition at position +5 of intron 46. This mutation creates a *Nla*III restriction site, thus facilitating the screening of a large number of chromosomes from control and affected populations.

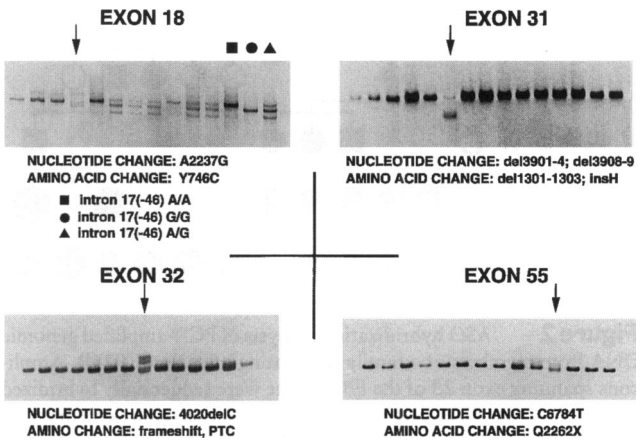

Figure 1 Representative heteroduplex-analysis gels showing band shifts that manifest either heterozygous mutations (*arrows*) or polymorphic sequence variants (exon 18). The nature of the nucleotide and amino acid changes are shown below each panel.

While this mutation was not present in 104 chromosomes from unaffected and unrelated individuals, the screening of 184 chromosomes from unrelated individuals with MFS resulted in the observation of a third recurrence in yet another patient with sporadic and classic disease (fig. 3*a*). While family members for one proband were unavailable for study, the other two occurrences of this mutation were demonstrated to be de novo events (fig. 3*b*). The substitution of the highly conserved G at position +5 of the mammalian consensus splice donor site is predicted to cause exon skipping (Shapiro and Senapathy 1987). Indeed, RT-PCR analysis of *FBN1* transcript from cultured fibroblasts from one of the probands revealed the in-frame skipping of exon 46 (fig. 3*c*). In addition, a small amount of abnormally spliced transcripts utilized a cryptic splice donor contained within exon 45 and a cryptic splice acceptor within exon 48 (fig. 3*d*). The only evident predisposition for this recurrent mutation is that it occurs at a CpG dinucleotide and is consistent with deamination of 5-methyl cytosine on the noncoding strand.

Discussion

Despite 3 years of intensive investigation of patients with MFS, to date a total of only 53 *FBN1* mutations, including the 15 discussed here, have been reported (Dietz et al. 1991*a*, 1992*a*, 1992*b*, 1993*a*, 1993*b*; Kainulainen et al. 1992, 1994; Hewett et al. 1993, 1994*b*; Tynan et al. 1993; Hayward et al. 1994*a*, 1994*b*; Kartunnen et al. 1994; Piersall et al. 1994; Stahl-Hallengren et al. 1994). This low number manifests low sensitivity (~10%) for previously employed RT-PCR–based screening methods. We now show that up to ~80% of mutations in unselected patients with classic MFS can

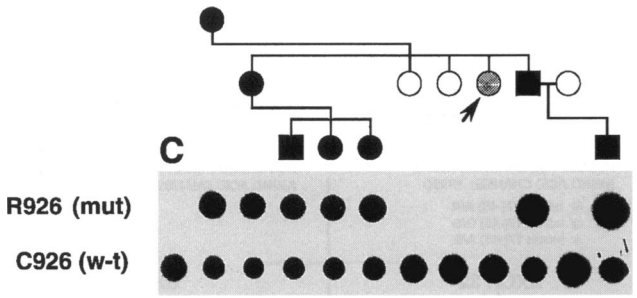

Figure 2 ASO hybridization analysis of PCR-amplified genomic DNA from members of a family segregating mutation C926R. Amplicons spanning exon 23 of the *FBN1* gene were sequentially hybridized to radiolabeled oligonucleotides that were either complementary to the mutant ("mut") allele sequence (R926) or the wild-type ("w-t") allele sequence (C926). "C" represents an unrelated and unaffected control. Circles represent females, and squares represent males. Unblackened symbols represent unaffected subjects; blackened symbols represent subjects affected with classic MFS; stippled symbol (*arrow*) represents an individual who satisfied the diagnostic criteria for MFS (Beighton et al. 1988) but, unlike other affected family members, had none of the "major" manifestations that are associated with this disease phenotype (Beighton et al. 1988).

be characterized using heteroduplex analysis of genomic amplicons.

While precise determination of the increase in efficiency afforded by our screening method awaits experience with a larger number of patients, it is interesting to consider which factors may account for the increased sensitivity that we have observed. From the outset, a dominant-negative effect of mutant protein upon its wild-type counterpart (Herskowitz 1987) seemed the likely pathogenesis for MFS, a prototypical autosomal dominant connective tissue disorder. It was therefore not intuitive that PTC mutants—specifically, those associated with extremely low levels of mutant transcript and protein—would contribute significantly to the etiology of this disorder. With the biochemical demonstration of impaired matrix utilization of wild-type protein (Milewicz et al. 1992; Aoyama et al. 1993, 1994), the identification of low-transcript mutations associated with MFS (Dietz et al. 1993*a*, 1993*b*), the realization that low message levels from one *FBN1* allele is not an uncommon finding in MFS patient samples (Hewett et al. 1994*a*), and the appreciation that even highly truncated monomers can exert a dominant-negative effect (Eldadah et al. 1995), this rationale had to be reexamined.

It seemed likely that the screening of amplicons derived from a genomic DNA template would provide an improved method to detect mutations. First, such procedures eliminate the need for a tissue source of *FBN1* mRNA. Second, if one excludes the possibility of large deletions, both alleles should be equally represented as templates for PCR despite the presence of mutations associated with low transcript levels. Indeed, using RT-PCR–based methods of screening, only 3 (8%) of 37 identified mutations were shown to decrease mutant transcript stability (Dietz et al. 1993*a*, 1993*b*). In contrast, 4 (28%) of 15 of mutations described here are predicted to alter mutant transcript abundance. Finally, the generation of amplicons spanning each exon using our primer set yields an average DNA fragment size of 250 bp, much shorter than that previously employed in our RT-PCR–based methods (Dietz et al. 1991*a*). It has been suggested that efficiency of heteroduplex analysis on MDE gels is less susceptible to DNA fragment size than other methods including SSCP (E. Highsmith, personal communication). Although we have not systematically compared SSCP and heteroduplex analysis with all other factors remaining constant, we have shown that single-condition heteroduplex analysis of relatively small amplicons generated from genomic DNA templates provides an efficient means to identify *FBN1* mutations causing MFS.

With one exception (Dietz et al. 1991*a*), all previously characterized mutations were specific to single families. This is true of 14 of 15 mutations described here. In contrast, a newly identified splice-site mutation, substitution of the highly conserved G at position +5 of intron 46 (Shapiro and Senapathy 1987), was found as a de novo event in three unrelated individuals. While there was no apparent predisposition for the other recurrent mutation, this novel mutation manifests a C-to-T transition within a CpG dinucleotide on the noncoding strand.

The majority of missense mutations causing MFS, including eight of nine described here, cluster within EGF-like domains (fig. 4). In addition, the majority of these mutations occur within 1 of the 43 EGF-like domains within fibrillin-1 that satisfy the consensus for calcium binding (Corson et al. 1993; Pereira et al. 1993), an event that may be necessary to stabilize tertiary structure, to promote protein-to-protein interactions, and to resist proteolysis (Cooke et al. 1987; Handford et al. 1991). Calcium binding to EGF-like domains is dependent on domain structure, as dictated by the three predictably spaced intradomain disulfide linkages and by a number of other highly conserved residues (Cooke et al. 1987; Stenflo et al. 1988; Dahlbäck et al. 1990; Handford et al. 1991; Selander-Sunnerhagen et al. 1992). The majority (9/16) of missense mutations within EGF-like domains that we have identified substitute cysteine residues and would therefore have an obligate effect on domain conformation (fig. 4). Of the remaining mutations, six of seven substitute residues important for calcium binding, including the highly conserved aspartic acid residue at domain position 2, the glutamic acid residue at position 5, the asparagine residue at position 10, and the aromatic tyrosine or phenylalanine residue at position 15. The arginine-to-proline mutation at posi-

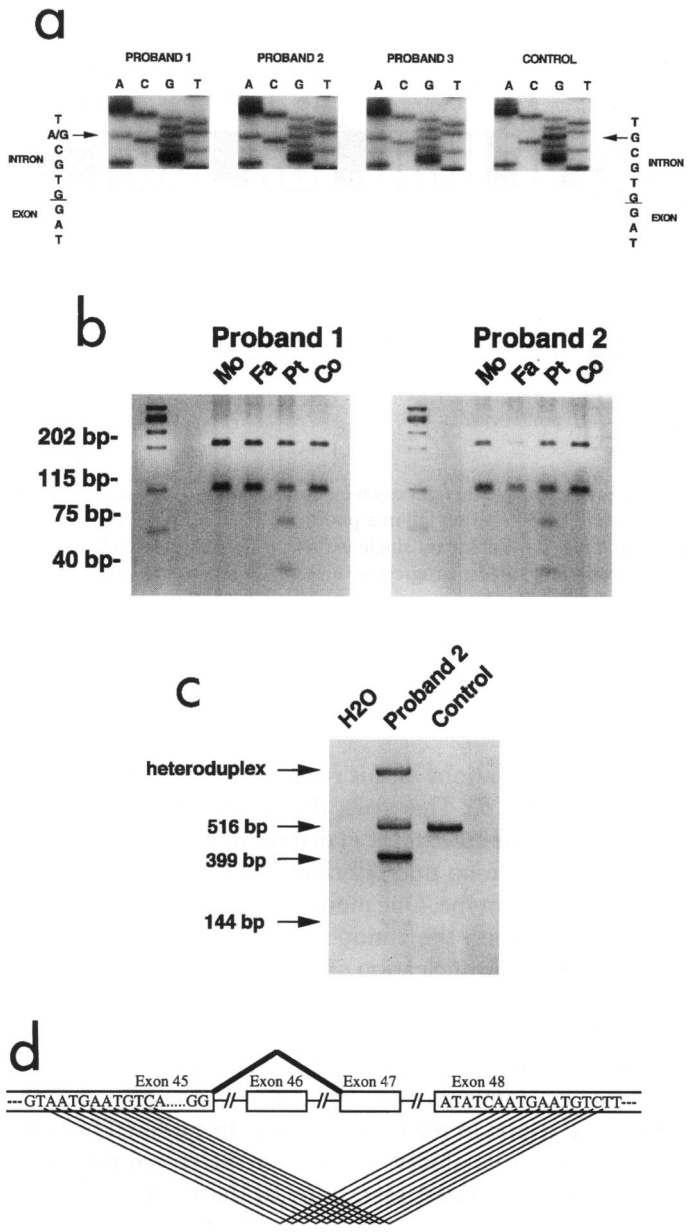

Figure 3 Identification and characterization of recurrent de novo mutation intron 46 G+5 to A. *a,* Direct sequence analysis of PCR-amplified genomic DNA, spanning exon 46 of the *FBN1* gene, from three unrelated probands with classic MFS and from an unaffected control individual. All three probands are heterozygous for A/G at position +5 of intron 46, while the control is homozygous for G (*arrows*). *b,* Restriction analysis of amplicons from probands 1 and 2 ("Pt"), their mothers ("Mo") and fathers ("Fa"), and unrelated and unaffected control individuals ("Co"). The mutation creates a novel *Nla*III restriction site. Due to the presence of a constant *Nla*III site, the 317-bp PCR product is cut to 202-bp and 115-bp fragments in all individuals. The novel site created by the mutation manifests as additional 75-bp and 40-bp fragments. *c,* RT-PCR analysis of mRNA extracted from cultured skin fibroblasts from proband 2 and a control individual. Normal splicing of exons 45–48 yields a 516-bp band. In the patient sample, a 399-bp product manifests the skipping of exon 46. In addition, a faint 144-bp band is seen in the patient sample, apparently because of the use of a cryptic splice donor in exon 45 and a cryptic splice acceptor in exon 48. The increased intensity of the 399-bp band relative to the 516-bp band was reproducible and probably reflects a difference in relative efficiency of amplification due to interval size and/or secondary structure. *d,* Cartoon depicting the abnormal splicing induced by mutation intron 46 G+5 to A. The major splice variant (*bold lines*) skips exon 46. While the minor splice variant manifests the use of cryptic sites in exons 45 and 48, one cannot distinguish between the multiple combinations of potential cryptic sites (*thin lines*) because of sequence redundancy in these regions. Note that none of the potential sites match the GT/AG mammalian consensus donor/acceptor sites, respectively (Shapiro and Senapathy 1987). Although false priming of a short extension product due to sequence redundancy cannot be excluded, the absence of this product in the control sample makes this less likely.

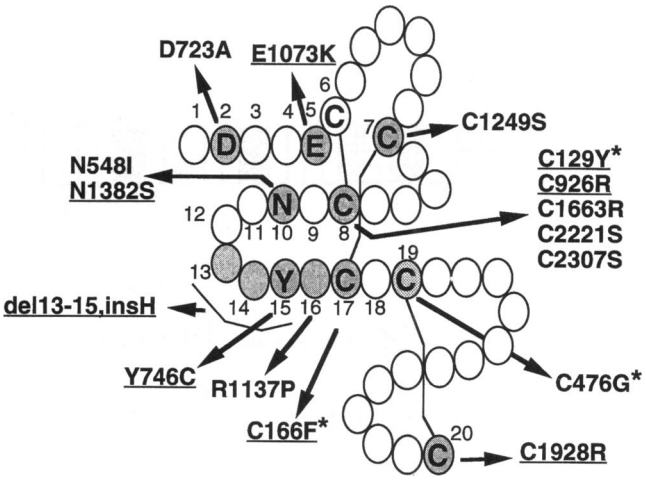

Figure 4 *FBN1* EGF-like domain consensus modeled after the solution structure of native EGF (Cooke et al. 1987). Residues with putative significance for calcium binding (Handford et al. 1991; Selander-Sunnerhagen et al. 1992) are numbered sequentially for each repeat. Amino acids that have been substituted by naturally occurring mutations in MFS are stippled. The sites of specific mutations are indicated by arrows. Bold lines indicate disulfide linkages between cysteine (C) residues. 1–5 are negatively charged amino terminal residues; 6–8, 17, 19, and 20 are highly conserved cysteine residues; 8–19 are the β-hydroxylase consensus sequence; 10 is the β-hydroxylated asparagine (N); and 15 is aromatic tyrosine (Y or F) residue. Underlined mutations are newly identified in this study. Asterisks (*) denote mutations that occur in EGF-like domains that do not satisfy the calcium-binding consensus. This figure is modified from one that has appeared elsewhere (Dietz et al. 1993*a*).

tion 16 (fig. 4) is less easily categorized. While arginine is often found at this position in *FBN1* EGF-like domains, it is not absolutely conserved. Recent characterization of the NMR-structure of this domain in both its wild-type (arginine) and mutant (proline) form at position 16 demonstrated that the mutant domain folds abnormally (Wu et al. 1995). The three mutations that occur within EGF-like domains that do not satisfy the calcium-binding consensus (fig. 4) all substitute highly

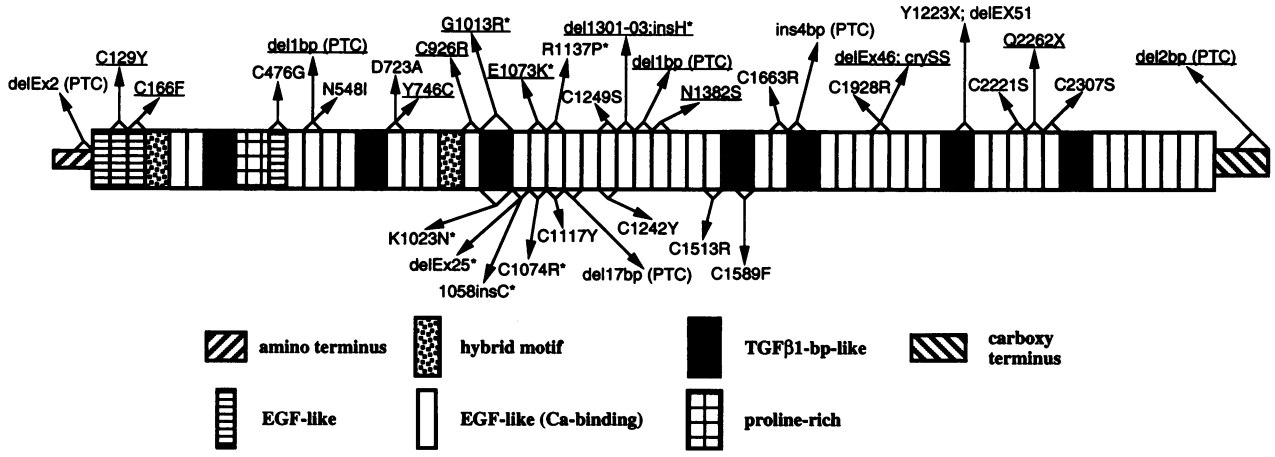

Figure 5 Mutations causing MFS superimposed on a cartoon showing the complete domain organization of *FBN1* (Corson et al. 1993; Pereira et al. 1993). All mutations that we have identified and mutations reported by others that fall in a putative critical region of the molecule (see text) are shown above and below the diagram, respectively. Triangular brackets encompass single exons. Mutations newly identified in this study are underlined. Those associated with infantile presentation of severe and rapidly progressive disease are denoted by asterisks (*). "PTC" denotes mutations that create a PTC.

conserved cysteine residues. The one new mutation that occurs within a TGF-β1-BP–like domain substitutes a glycine residue that is conserved in six of seven such domains in fibrillin-1 and all three such domains in TGF-β1-BP (Maslen et al. 1991; Corson et al. 1993; Pereira et al. 1993). The functional implications for substitution of this highly conserved residue remain unknown.

Although fibrillin-1 mutations causing MFS appear equally distributed along the length of the protein (fig. 5), Kainulainen et al. (1994) first noticed that mutations causing a severe neonatal presentation of rapidly progressive disease appear to cluster within a relatively confined region of fibrillin-1, extending from third TGF-β1-BP–like domain (numbered from the amino terminus) to the third downstream EGF-like domain (exons 24–27). Furthermore, it was suggested that the location of the mutation, rather than its character, might be the more influential factor in determining phenotypic severity. Our present data both confirm and extend this correlation of phenotype to genotype. While one mutation associated with neonatal presentation of severe and rapidly progressive skeletal involvement localized to exon 4, far removed from the putative critical region, the cardiovascular involvement was relatively mild. Three of our mutations causing the "complete" severe phenotype fell in exons 24, 26, and 27. A fourth localized to exon 31, thus extending the region associated with the most severe spectrum of disease in a 3′ direction. This region encodes a long and uninterrupted stretch of EGF-like motifs that may be structurally interdependent due to the formation of a common β sheet between adjacent domains (Mosher et al. 1992; Pereira et al. 1993). It is therefore probable that selected mutations in this region can structurally perturb the monomer over a wide distance.

Many mutations in this region, however, lead to classic MFS (fig. 5). Therefore, the position of the mutation cannot be the sole factor in determining the consequence of a mutation on microfibrillar assembly and hence the disease phenotype. One model of microfibrillar assembly holds that both the amino and carboxy termini are influential in the nucleation of fibrillin-1 monomers during aggregation (Sakai et al. 1991; Eldadah et al. 1995) Monomers that are most structurally perturbed at these ends would be least able to disrupt microfibrillar assembly via a dominant-negative effect. We suggest that the central region of the monomer may be buffered by other domains in its ability to transmit the structural consequences of selected mutations to the termini. If valid, mutations that cause minimal or "bufferable" perturbation of local structure within this central region would result in the most devastating phenotype. If one focuses on the region flanked by TGF-β1-BP–like domains 3 and 4 (numbered from the amino terminus), five of seven mutations associated with a milder phenotype substitute cysteine residues. Such mutations would be expected to have severe structural consequences due to obligate perturbation of intradomain disulfide linkages, the presence of free sulfhydryl groups, or both. The other two mutations associated with milder disease create PTCs that are predicted to have a minimized effect on microfibrillogenesis because of the lack of a translated carboxy terminus and/or low levels of mutant transcript and protein. In contrast, seven of eight mutations causing the severe and rapidly progressive phenotype represent either noncysteine substitutions or in-frame deletions or

insertions (Kainulainen et al. 1994; Milewicz et al. 1994). Only one causes the substitution of a conserved cysteine residue. While this correlation between class of mutation and phenotypic severity appears highly significant ($P = .0012$; Fisher's exact test), the study of many more mutations will be necessary to evaluate this proposed interrelation of structure, function and phenotype.

In conjunction with a highly informative panel of intragenic microsatellite polymorphisms (Pereira et al. 1994), the requisite tools are now available to directly address the issue of locus heterogeneity in MFS. Such efforts will not only promote scientific inquiry but will have an immediate impact on the ability to perform presymptomatic diagnosis. This is exemplified by the family segregating mutation C926R where direct mutational analysis confirmed that an "affected" individual with atypically mild features did not inherit the mutant allele associated with classic disease in her extended family (fig. 2). While haplotype segregation analysis for this family reached an identical conclusion, direct mutational analysis is uniquely suitable for the study of small families or sporadic cases.

While locus heterogeneity in MFS appears unlikely, the extreme clinical variability inherent to this disorder manifests the concerted influence of a heterogeneous set of variables on the expression of, and reaction to, the primary etiologic agent. Only on the identification of many mutations in *FBN1,* and the subsequent correlation of genotype to phenotype, can one begin to consider the dynamic interplay between mutant *FBN1* genotype and epistatic, stochastic, and environmental modifiers.

Acknowledgments

We thank Linda Piersall and Mark Clough for technical assistance, and Drs. S. Black, S. Fallet, D. Chitayat and P. Kaplan for supplying patient samples and clinical information. Major support for this work was provided by the Kyle Mann Fund of the National Marfan Foundation. Also supported in part by NIH grants HL-02815 (to H.C.D.), AR-41135 (to C.A.F.), HL-35877 (to R.E.P.), RR00722 (Outpatient General Research Centers Grant), HD24061 (Cell Culture Core Facility), and a predoctoral minority fellowship from the NIGMS (to G.N.); by the American Heart Association (New York City Affiliate, to F.R.); by the Dr. Amy and James Elster Research Fund (to F.R.); by the Simon family (to C.A.F.); and by the Smilow Foundation (to H.C.D.). H.C.D. is a Richard Starr Ross Research Scholar.

References

Aoyama T, Francke U, Dietz HC, Furthmayr H (1994) Quantitative differences in biosynthesis and extracellular deposition of fibrillin in cultured fibroblasts distinguish five groups of Marfan syndrome patients and suggest distinct pathogenetic mechanisms. J Clin Invest 94:130–137

Aoyama T, Tynan K, Dietz HC, Francke U, Furthmayr H (1993) Missense mutations impair intracellular processing of fibrillin and microfibril assembly in Marfan syndrome. Hum Mol Genet 2:2135–2140

Beighton P, de Paepe A, Danks D, Finidori G, Gedde-Dahl T, Goodman R, Hall JG, et al (1988) International Nosology of Heritable Disorders of Connective Tissue, Berlin, 1986. Am J Med Genet 29:581–594

Byers PH (1993) Second international symposium on the Marfan syndrome, November 7–9, 1992, San Francisco. Hum Mutat 2:80–81

Cheng J, Fogel-Petrovic M, Maquat LE (1990) Translation to near the distal end of the penultimate exon is required for normal levels of spliced triosephosphate isomerase mRNA. Mol Cell Biol 10:5215–5225

Collod G, Babron M-C, Jondeau G, Coulon M, Weissenbach J, Dubourg O, Bourdarias J-P, et al (1994) A second locus for Marfan syndrome maps to chromosome 3p24.2-p25. Nat Genet 8:264–268

Cooke RM, Wilkinson AJ, Baron M, Pastore A, Tappin MJ, Campbell ID, Gregory H, et al (1987) The solution structure of human epidermal growth factor. Nature 327:339–341

Corson GM, Chalberg SC, Dietz HC, Charbonneau NL, Sakai LY (1993) Fibrillin binds calcium and is coded by cDNAs that reveal a multidomain structure and alternatively spliced exons at the 5′ end. Genomics 17:476–484

Dahlbäck B, Hildebrand B, Linse S (1990) Novel type of very high affinity calcium binding sites in β-hydroxyasparagine-containing epidermal growth factor-like domains in vitamin K-dependent protein S. J Biol Chem 265:18481–18489

Dietz HC, Cutting GR, Pyeritz RE, Maslen CL, Sakai LY, Corson GM, Puffenberger EG, et al (1991*a*) Marfan syndrome caused by a recurrent de novo missense mutation in the fibrillin gene. Nature 352:337–339

Dietz HC, Francke U, Furthmayr H, Francomano C, De Paepe A, Devereux R, Ramirez F, Pyeritz R (1995) The question of heterogeneity in Marfan syndrome). Nat Genet 9:228–229

Dietz HC, McIntosh I, Sakai LY, Corson GM, Chalberg SC, Pyeritz RE, Francomano CA (1993*a*) Four novel *FBN1* mutations: significance for mutant transcript level and EGF-like domain calcium binding in the pathogenesis of Marfan syndrome. Genomics 17:468–475

Dietz HC, Pyeritz RE, Hall BD, Cadle RG, Hamosh A, Schwartz J, Meyers DA, et al (1991*b*) The Marfan syndrome locus: confirmation of assignment to chromosome 15 and identification of tightly linked markers at 15q15-q21.3. Genomics 9:355–361

Dietz HC, Pyeritz RE, Puffenberger EG, Kendzior RJ Jr, Corson GM, Maslen CL, Sakai LY, et al (1992*a*) Marfan phenotype variability in a family segregating a missense mutation in the epidermal growth factor-like motif of the fibrillin gene. J Clin Invest 89:1674–1680

Dietz HC, Saraiva JM, Pyeritz RE, Cutting GR, Francomano CA (1992*b*) Clustering of fibrillin (*FBN1*) missense mutations in Marfan syndrome patients at cysteine residues in EGF-like domains. Hum Mutat 1:366–374

Dietz HC, Valle D, Francomano CA, Kendzior RJ Jr, Pyeritz

RE, Cutting GR (1993*b*) The skipping of constitutive exons in vivo induced by nonsense mutations. Science 259:680–683

Eldadah ZA, Brenn T, Furthmayr H, Dietz HC (1995) Expression of a mutant fibrillin (*FBN1*) allele upon a normal human or murine genetic background recapitulates a Marfan cellular phenotype. J Clin Invest 95:874–880

Godfrey M, Menashe V, Weleber RG, Koler RD, Bigley RH, Lovrien E, Zonana J, et al (1990) Cosegregation of elastin-associated microfibrillar abnormalities with the Marfan phenotype in families. Am J Hum Genet 46:652–660

Godfrey M, Vandemark N, Wang M, Velinov M, Wargowski D, Tsipouras P, Han J, et al (1993) Prenatal diagnosis and a donor splice site mutation in fibrillin in a family with Marfan syndrome. Am J Hum Genet 53:472–480

Handford PA, Mayhew M, Baron M, Winship PR, Campbell ID, Brownlee GG (1991) Key residues involved in calcium binding motifs in EGF-like domains. Nature 351:164–167

Hayward C, Porteous ME, Brock DJ (1994*a*) Identification of a novel nonsense mutation in the fibrillin gene (*FBN1*) using nonisotopic techniques. Hum Mutat 3:159–62

Hayward C, Rae AL, Porteous ME, Logie LJ, Brock DJ (1994*b*) Two novel mutations and a neutral polymorphism in EGF-like domains of the fibrillin gene (*FBN1*): SSCP screening of exons 15–21 in Marfan syndrome patients. Hum Mol Genet 3:373–375

Herskowitz I (1987) Functional inactivation of genes by dominant negative mutations. Nature 329:219–222

Hewett DR, Lynch J, Child A, Firth H, Sykes B (1994*a*) Differential allelic expression of a fibrillin gene (*FBN1*) in patients with Marfan syndrome. Am J Hum Genet 55:447–452

Hewett DR, Lynch JR, Child A, Sykes BC (1994*b*) A new missense mutation of fibrillin in a patient with Marfan syndrome. J Med Genet 31:338–339

Hewett DR, Lynch JR, Smith R, Sykes BC (1993) A novel fibrillin mutation in the Marfan syndrome which could disrupt calcium binding of the epidermal growth factor-like module. Hum Mol Genet 2:475–477

Hollister DW, Godfrey M, Sakai LY, Pyeritz RE (1990) Immunohistologic abnormalities of the microfibrillar-fiber system in the Marfan syndrome. N Engl J Med 323:152–159

Kainulainen K, Karttunen L, Puhakka L, Sakai L, Peltonen L (1994) Mutations in the fibrillin gene responsible for dominant ectopia lentis and neonatal Marfan syndrome. Nat Genet 6:64–69

Kainulainen K, Pulkkinen L, Savolainen A, Kaitila I, Peltonen L (1990) Location on chromosome 15 of the gene defect causing Marfan syndrome. N Engl J Med 323:935–939

Kainulainen K, Sakai LY, Child A, Pope FM, Puhakka L, Ryhanen L, Palotie A, Kaitila I, Peltonen L (1992) Two mutations in Marfan syndrome resulting in truncated fibrillin polypeptides. Proc Natl Acad Sci USA 89:5917–5921

Kainulainen K, Steinmann B, Collins F, Dietz HC, Francomano CA, Child A, Kilpatrick MW, et al (1991) Marfan syndrome: no evidence for heterogeneity in different populations, and more precise mapping of the gene. Am J Hum Genet 49:662–667

Kartunnen L, Raghunath M, Lönnqvist L, Peltonen L (1994) A compound heterozygous Marfan patient: two defective fibrillin alleles result in a lethal phenotype. Am J Hum Genet 55:1083–1091

Kielty CM, Phillips JE, Child AH, Pope FM, Shuttleworth CA (1994) Fibrillin secretion and microfibril assembly by Marfan dermal fibroblasts. Matrix Biol 14:191–199

Lee B, Godfrey M, Vitale E, Hori H, Mattei MG, Sarfarazi M, Tsipouras P, et al (1991) Linkage of Marfan syndrome and a phenotypically related disorder to two different fibrillin genes. Nature 352:330–334

Maslen CL, Corson GM, Maddox BK, Glanville RW, Sakai LY (1991) Partial sequence of a candidate gene for the Marfan syndrome. Nature 352:334–337

Milewicz DM, Duvic M (1994) Severe neonatal Marfan syndrome resulting from a de novo 3-bp insertion into the fibrillin gene on chromosome 15. Am J Hum Genet 54:447–453

Milewicz DM, Pyeritz RE, Crawford ES, Byers PH (1992) Marfan syndrome: defective synthesis, secretion, and extracellular matrix formation of fibrillin by cultured dermal fibroblasts. J Clin Invest 89:79–86

Mosher DF, Sottile J, Wu C, McDonald JA (1992) Assembly of extracellular matrix. Cell Biol 4:810–818

Pereira L, D'Alessio M, Ramirez F, Lynch JR, Sykes B, Pangilinan T, Bonadio J (1993) Genomic organization of the sequence coding for fibrillin, the defective gene product in Marfan syndrome. Hum Mol Genet 2:961–968

Pereira L, Levran O, Ramirez F, Lynch JR, Sykes B, Pyeritz RE, Dietz HC (1994) Diagnosis of Marfan syndrome: a molecular approach to the stratification of cardiovascular risk within families with Marfan's syndrome. N Engl J Med 331:148–153

Piersall LD, Dietz HC, Hall BD, Cadle RG, Pyeritz RE, Francomano CA, McIntosh I (1994) Substitution of a cysteine residue in a non-calcium binding, EGF-like domain of fibrillin segregates with the Marfan syndrome in a large kindred. Hum Mol Genet 3:1013–1014

Pyeritz RE, Francke U (1993) The Second International Symposium on the Marfan Syndrome. Am J Med Genet 47:127–135

Ravnik-Glavac M, Glavac D, Dean M (1994) Sensitivity of single-strand conformation polymorphism and heteroduplex method for mutation detection in the cystic fibrosis gene. Hum Mol Genet 3:801–807

Sakai LY, Keene DR, Engvall E (1986) Fibrillin, a new 350-kD glycoprotein, is a component of extracellular microfibrils. J Cell Biol 103:2499–2509

Sakai LY, Keene DR, Glanville RW, Bachinger HP (1991) Purification and partial characterization of fibrillin, a cysteine-rich structural component of connective tissue microfibrils. J Biol Chem 266:14763–14770

Sarfarazi M, Tsipouras P, Del Mastro R, Kilpatrick M, Farndon P, Boxer M, Bridges A, et al (1992) A linkage map of 10 loci flanking the Marfan syndrome locus on 15q: results of an international consortium study. J Med Genet 29:75–80

Selander-Sunnerhagen M, Ullner M, Persson E, Teleman O, Stenflo J, Drakenberg T (1992) How an epidermal growth factor (EGF)-like domain binds calcium. J Biol Chem 267:19642–19649

Shapiro MB, Senapathy P (1987) RNA splice junctions of dif-

ferent classes of eukaryotes: sequence statistics and functional implications in gene expression. Nucleic Acids Res 15:7155–7174

Stahl-Hallengren C, Ukkonen T, Kainulainen K, Kristofersson U, Saxne T, Tornqvist K, Peltonen L (1994) An extra cysteine in one of the non-calcium-binding epidermal growth factor-like motifs of the *FBN1* polypeptide is connected to a novel variant of Marfan syndrome. J Clin Invest 94:709–713

Stenflo J, Öhlin A-K, Owen WG, Schneider WJ (1988) β-hydroxyaspartic acid or β-hydroxyasparagine in bovine low density lipoprotein receptor and in bovine thrombomodulin. J Biol Chem 263:21–24

Sykes B (1993) Marfan gene dissected. Nat Genet 3:99–100

Tsipouras P, Del Mastro R, Sarfarazi M, Lee B, Vitale E, Child AH, Godfrey M, et al (1992) Genetic linkage of the Marfan syndrome, ectopia lentis, and congenital contractural arachnodactyly to the fibrillin genes on chromosomes 15 and 5: The International Marfan Syndrome Collaborative Study. N Engl J Med 326:905–909

Tsipouras P, Sarfarazi M, Devi A, Weiffenbach B, Boxer M (1991) Marfan syndrome is closely linked to a marker on chromosome 15q1.5 to q2.1. Proc Natl Acad Sci USA 88:4486–4488

Tynan K, Comeau K, Pearson M, Wilgenbus P, Levitt D, Gasner C, Berg MA, et al (1993) Mutation screening of complete fibrillin-1 coding sequence: report of five new mutations, including two in 8-cysteine domains. Hum Mol Genet 2:1813–1821

Urlaub G, Mitchell PJ, Ciudad CJ, Chasin LA (1989) Nonsense mutations in the dihydrofolate reductase gene affect RNA processing. Mol Cell Biol 9:2868–2880

Wu Y-S, Bevilacqua VLH, Berg JM. Fibrillin domain folding and calcium binding: significance to Marfan syndrome (1995) Chem Biol 2:91–97